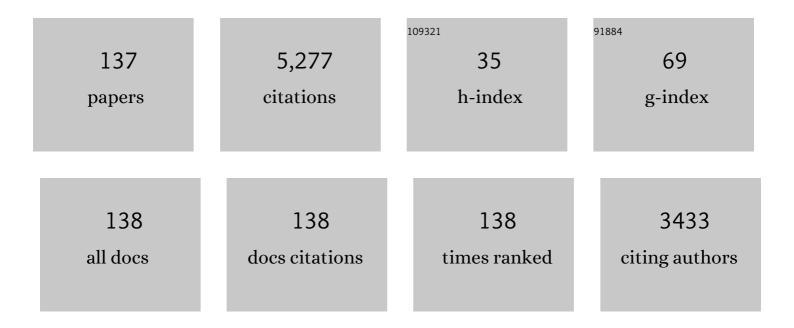
List of Publications by Year in descending order

Source: https://exaly.com/author-pdf/3736591/publications.pdf Version: 2024-02-01



#	Article	IF	CITATIONS
1	Graphene-based passively Q-switched dual-wavelength erbium-doped fiber laser. Optics Letters, 2010, 35, 3709.	3.3	461
2	106μm Q-switched ytterbium-doped fiber laser using few-layer topological insulator Bi_2Se_3 as a saturable absorber. Optics Express, 2013, 21, 29516.	3.4	319
3	1-, 1.5-, and 2-μm Fiber Lasers Q-Switched by a Broadband Few-Layer MoS ₂ Saturable Absorber. Journal of Lightwave Technology, 2014, 32, 4679-4686.	4.6	318
4	Mid-infrared integrated photonics on silicon: a perspective. Nanophotonics, 2017, 7, 393-420.	6.0	280
5	Two-dimensional material-based saturable absorbers: towards compact visible-wavelength all-fiber pulsed lasers. Nanoscale, 2016, 8, 1066-1072.	5.6	246
6	Nonlinear optical absorption of few-layer molybdenum diselenide (MoSe_2) for passively mode-locked soliton fiber laser [Invited]. Photonics Research, 2015, 3, A79.	7.0	227
7	Chalcogenide glass-on-graphene photonics. Nature Photonics, 2017, 11, 798-805.	31.4	190
8	Widely-tunable, passively Q-switched erbium-doped fiber laser with few-layer MoS_2 saturable absorber. Optics Express, 2014, 22, 25258.	3.4	183
9	Passively Q-switched Nd:YAlO_3 nanosecond laser using MoS_2 as saturable absorber. Optics Express, 2014, 22, 28934.	3.4	123
10	Evanescent-Light Deposition of Graphene Onto Tapered Fibers for Passive Q-Switch and Mode-Locker. IEEE Photonics Journal, 2012, 4, 1295-1305.	2.0	118
11	Preparation of Few-Layer Bismuth Selenide by Liquid-Phase-Exfoliation and Its Optical Absorption Properties. Scientific Reports, 2014, 4, 4794.	3.3	112
12	Ultrathin GeSe Nanosheets: From Systematic Synthesis to Studies of Carrier Dynamics and Applications for a High-Performance UV–Vis Photodetector. ACS Applied Materials & Interfaces, 2019, 11, 4278-4287.	8.0	105
13	Graphdiyneâ€Polymer Nanocomposite as a Broadband and Robust Saturable Absorber for Ultrafast Photonics. Laser and Photonics Reviews, 2020, 14, 1900367.	8.7	99
14	Topological-Insulator Passively Q-Switched Double-Clad Fiber Laser at 2 <formula formulatype="inline"> <tex notation="TeX">\$mu\$</tex>m Wavelength. IEEE Journal of Selected Topics in Quantum Electronics, 2014, 20, 1-8.</formula 	2.9	86
15	High-energy passively Q-switched 2 μm Tm^3+-doped double-clad fiber laser using graphene-oxide-deposited fiber taper. Optics Express, 2013, 21, 204.	3.4	84
16	Gold nanoparticles as a saturable absorber for visible 635 nm Q-switched pulse generation. Optics Express, 2015, 23, 24071.	3.4	80
17	Chip-scale broadband spectroscopic chemical sensing using an integrated supercontinuum source in a chalcogenide glass waveguide. Photonics Research, 2018, 6, 506.	7.0	78
18	Topological insulator Bi_2Se_3 based Q-switched Nd:LiYF_4 nanosecond laser at 1313 nm. Optics Express, 2015, 23, 7674.	3.4	76

#	Article	IF	CITATIONS
19	Graphene-Induced Nonlinear Four-Wave-Mixing and Its Application to Multiwavelength Q-Switched Rare-Earth-Doped Fiber Lasers. Journal of Lightwave Technology, 2011, 29, 2732-2739.	4.6	70
20	A self-powered photodetector based on two-dimensional boron nanosheets. Nanoscale, 2020, 12, 5313-5323.	5.6	60
21	12-W average-power, 700-W peak-power, 100-ps dissipative soliton resonance in a compact Er:Yb co-doped double-clad fiber laser. Optics Letters, 2017, 42, 462.	3.3	59
22	Diode-pumped Pr^3+:LiYF_4 continuous-wave deep red laser at 698Ânm. Journal of the Optical Society of America B: Optical Physics, 2013, 30, 302.	2.1	58
23	Multiwavelength Dissipative-Soliton Generation in Yb-Fiber Laser Using Graphene-Deposited Fiber-Taper. IEEE Photonics Technology Letters, 2012, 24, 1539-1542.	2.5	56
24	High-order mode direct oscillation of few-mode fiber laser for high-quality cylindrical vector beams. Optics Express, 2018, 26, 11850.	3.4	56
25	Direct generation of watt-level yellow Dy ³⁺ -doped fiber laser. Photonics Research, 2021, 9, 446.	7.0	55
26	Towards visible-wavelength passively mode-locked lasers in all-fibre format. Light: Science and Applications, 2020, 9, 61.	16.6	52
27	Ultraâ€Small 2D PbS Nanoplatelets: Liquidâ€Phase Exfoliation and Emerging Applications for Photoâ€Electrochemical Photodetectors. Small, 2021, 17, e2005913.	10.0	50
28	Graphene-Assisted Multiwavelength Erbium-Doped Fiber Ring Laser. IEEE Photonics Technology Letters, 2011, 23, 501-503.	2.5	44
29	Orange-light passively Q-switched Pr^3+-doped all-fiber lasers with transition-metal dichalcogenide saturable absorbers. Optical Materials Express, 2016, 6, 2031.	3.0	42
30	2 Âμm high-power dissipative soliton resonance in a compact Ϊƒ-shaped Tm-doped double-clad fiber laser. Applied Physics Express, 2018, 11, 052701.	2.4	41
31	Determining topological charge based on an improved Fizeau interferometer. Optics Express, 2019, 27, 12774.	3.4	41
32	Dynamic mode-switchable optical vortex beams using acousto-optic mode converter. Optics Letters, 2018, 43, 5841.	3.3	40
33	Passively Mode-Locked Tm3+-Doped Fiber Laser With Gigahertz Fundamental Repetition Rate. IEEE Journal of Selected Topics in Quantum Electronics, 2018, 24, 1-6.	2.9	38
34	635-nm Visible Pr3+-Doped ZBLAN Fiber Lasers Q-Switched by Topological Insulators SAs. IEEE Photonics Technology Letters, 2015, 27, 2379-2382.	2.5	36
35	Efficient continuous-wave and short-pulse Ho ³⁺ -doped fluorozirconate glass all-fiber lasers operating in the visible spectral range. Nanoscale, 2018, 10, 5272-5279.	5.6	36
36	Direct generation of an ultrafast vortex beam in a CVD-graphene-based passively mode-locked Pr:LiYF ₄ visible laser. Photonics Research, 2019, 7, 1209.	7.0	36

#	Article	IF	CITATIONS
37	Bidirectional operation of 100 fs bound solitons in an ultra-compact mode-locked fiber laser. Optics Express, 2016, 24, 21020.	3.4	33
38	Passive Q-Switching of a Diode-Pumped Pr:LiYF ₄ Visible Laser Using WS ₂ as Saturable Absorber. IEEE Photonics Journal, 2016, 8, 1-6.	2.0	33
39	Compact Passive Q-Switching Pr3+-Doped ZBLAN Fiber Laser With Black Phosphorus-Based Saturable Absorber. IEEE Journal of Selected Topics in Quantum Electronics, 2017, 23, 7-12.	2.9	33
40	Self-Q-switched and wavelength-tunable tungsten disulfide-based passively Q-switched Er:Y ₂ O ₃ ceramic lasers. Photonics Research, 2018, 6, 830.	7.0	30
41	High-efficiency, yellow-light Dy ³⁺ -doped fiber laser with wavelength tuning from 5687 to 5819  nm. Optics Letters, 2019, 44, 4423.	3.3	30
42	MXene Ti ₃ C ₂ T _x saturable absorber for passively Q-switched mid-infrared laser operation of femtosecond-laser–inscribed Er:Y ₂ O ₃ ceramic channel waveguide. Nanophotonics, 2020, 9, 2495-2503.	6.0	29
43	212-kHz-linewidth, transform-limited pulses from a single-frequency Q-switched fiber laser based on a few-layer Bi ₂ Se ₃ saturable absorber. Photonics Research, 2018, 6, C29.	7.0	29
44	Ultralow-threshold cascaded Brillouin microlaser for tunable microwave generation. Optics Letters, 2015, 40, 4971.	3.3	28
45	Direct generation of 2  W average-power and 232  nJ picosecond pulses from an ultra-simple Yb double-clad fiber laser. Optics Letters, 2015, 40, 1097.	-doped	28
46	Stable, Ultrafast Pulse Mode-Locked by Topological Insulator <inline-formula> <tex-math notation="TeX">\${m Bi}_{2}{m Se}_{3} \$</tex-math </inline-formula> Nanosheets Interacting With Photonic Crystal Fiber: From Anomalous Dispersion to Normal Dispersion. IEEE Photonics Journal, 2015, 7, 1-8.	2.0	27
47	Visibleâ€Wavelength Spatiotemporal Mode‣ocked Fiber Laser Delivering 9 ps, 4 nJ Pulses at 635 nm. Laser and Photonics Reviews, 2022, 16, .	8.7	27
48	716  nm deep-red passively Q-switched Pr:ZBLAN all-fiber laser using a carbon-nanotube saturable absorber. Optics Letters, 2017, 42, 671.	3.3	26
49	Passive Synchronization of 1.06- and 1.53-(mu) m Fiber Lasers Q-switched by a Common Graphene SA. IEEE Photonics Technology Letters, 2014, 26, 1474-1477.	2.5	23
50	Compact self-Q-switched green upconversion Er:ZBLAN all-fiber laser operating at 5434  nm. Optics Letters, 2016, 41, 2258.	3.3	23
51	Bidirectional Red-Light Passively Q-Switched All-Fiber Ring Lasers With Carbon Nanotube Saturable Absorber. Journal of Lightwave Technology, 2018, 36, 2694-2701.	4.6	23
52	Real-time observation of vortex mode switching in a narrow-linewidth mode-locked fiber laser. Photonics Research, 2020, 8, 1203.	7.0	22
53	Simplified analytic solutions and a novel fast algorithm for Yb3+-doped double-clad fiber lasers. Optics Communications, 2007, 277, 118-124.	2.1	21
54	Stable and spacing-adjustable multiwavelength Raman fiber laser based on mixed- cascaded phosphosilicate fiber Raman linear cavity. Optics Letters, 2008, 33, 1602.	3.3	21

#	Article	IF	CITATIONS
55	Multiwavelength Fiber Optical Parametric Oscillator. IEEE Photonics Technology Letters, 2009, 21, 1609-1611.	2.5	21
56	Raman fiber laser harmonically mode-locked by exploiting the intermodal beating of CW multimode pump source. Optics Express, 2012, 20, 19905.	3.4	21
57	Emission properties and CW laser operation of Pr:YLF in the 910 nm spectral range. Optics Express, 2014, 22, 31722.	3.4	21
58	Numerical modeling of mid-infrared fiber optical parametric oscillator based on the degenerated FWM of tellurite photonic crystal fiber. Applied Optics, 2013, 52, 525.	1.8	20
59	High-Order Vortex Generation From CW and Passively Q-Switched Pr:YLF Visible Lasers. IEEE Photonics Technology Letters, 2019, 31, 1457-1460.	2.5	20
60	Visible-wavelength pulsed lasers with low-dimensional saturable absorbers. Nanophotonics, 2020, 9, 2273-2294.	6.0	20
61	CdTe/CdS Quantum Dots: Effective Saturable Absorber for Visible Lasers. IEEE Journal of Selected Topics in Quantum Electronics, 2017, 23, 1-7.	2.9	19
62	Green/red pulsed vortex-beam oscillations in all-fiber lasers with visible-resonance gold nanorods. Nanoscale, 2019, 11, 15991-16000.	5.6	19
63	Compact all-fiber 21-27 <i>μ</i> m tunable Raman soliton source based on germania-core fiber. Optics Express, 2019, 27, 28544.	3.4	19
64	Switchable and tunable multiple-channel erbium-doped fiber laser using graphene-polymer nanocomposite and asymmetric two-stage fiber Sagnac loop filter. Applied Optics, 2011, 50, 2940.	2.1	18
65	Self-mode-locked 2Âμm Tm ³⁺ -doped double-clad fiber laser with a simple linear cavity. Applied Optics, 2014, 53, 892.	1.8	18
66	MoS ₂ nano-flake doped polyvinyl alcohol enabling polarized soliton mode-locking of a fiber laser. Journal of Materials Chemistry C, 2016, 4, 9454-9459.	5.5	18
67	Unveiling the Stimulated Robust Carrier Lifetime of Surfaceâ€Bound Excitons and Their Photoresponse in InSe. Advanced Materials Interfaces, 2019, 6, 1900171.	3.7	18
68	2.01–2.42 <inline-formula> <tex-math notation="LaTeX">\$mu\$</tex-math> </inline-formula> m All-Fiber Femtosecond Raman Soliton Generation in a Heavily Germanium Doped Fiber. IEEE Journal of Selected Topics in Quantum Electronics, 2019, 25, 1-7.	2.9	18
69	Large-energy, wavelength-tunable, all-fiber passively Q-switched Er:Yb-codoped double-clad fiber laser with mono-layer chemical vapor deposition graphene. Applied Optics, 2014, 53, 4089.	1.8	17
70	Watt-level narrow-linewidth Nd:YAG laser operating on ^4F_3/2→^4I_15/2 transition at 1834 nm. Optics Express, 2016, 24, 3601.	3.4	17
71	High-performance SOA-based multiwavelength fiber lasers incorporating a novel double-pass waveguide-based MZI. Applied Physics B: Lasers and Optics, 2009, 96, 29-38.	2.2	16
72	Graphene mode-locked and Q-switched 2 - μ m Tm/Ho codoped fiber lasers using 1212-nm high-efficient pumping. Optical Engineering, 2016, 55, 081310.	1.0	16

#	Article	IF	CITATIONS
73	1.7-\$mu\$m Tm/Ho-Codoped All-Fiber Pulsed Laser Based on Intermode-Beating Modulation Technique. Journal of Lightwave Technology, 2018, 36, 4894-4899.	4.6	16
74	Incorporating MoS ₂ saturable absorption with nonlinear polarization rotation for stabilized mode-locking fibre lasers. Laser Physics Letters, 2018, 15, 075102.	1.4	16
75	Spectroscopic analysis of Pr3+:Gd3Ga5O12 crystal as visible laser material. Optical Materials, 2010, 33, 191-195.	3.6	15
76	Passively <inline-formula> <tex-math notation="LaTeX">\$Q\$ </tex-math> </inline-formula>-Switched Red Pr³⁺-Doped Fiber Laser With Graphene-Oxide Saturable Absorber. IEEE Photonics Technology Letters, 2016, 28, 1755-1758.</inline-formula>	2.5	15
77	Tunable and Selectable Multipassband Microwave Photonic Filter Utilizing Reflective and Cascaded Fiber Mach–Zehnder Interferometers. Journal of Lightwave Technology, 2017, 35, 2660-2668.	4.6	15
78	A few-layer InSe-based sensitivity-enhanced photothermal fiber sensor. Journal of Materials Chemistry C, 2020, 8, 132-138.	5.5	15
79	Intermode beating mode-locking technique for O-band mixed-cascaded Raman fiber lasers. Optics Letters, 2015, 40, 502. Nanosecond-Pulsed, Dual-Wavelength Passively Q-Switched c-Cut	3.3	14
80	Nd:YVO <inline-formula><tex-math>\$_{f 4}\$ </tex-math></inline-formula> Laser Using a Few-Layer Bi <inline-formula><tex-math>\$_{f 2}\$</tex-math></inline-formula> Se <inline-formula><tex-math>\$_{f 3}\$</tex-math></inline-formula> Saturable Absorber. IEEE Journal of Selected Topics in	2.9	14
81	Quantum Electronics, 2015, 21, 369-374. Single- and multi-wavelength Nd:YAlO3 lasers at 1328, 1339 and 1364nm. Optics and Laser Technology, 2016, 81, 1-6.	4.6	14
82	Sub-15-ns Passively Q-Switched Er:YSGG Laser at <inline-formula> <tex-math notation="LaTeX">\$2.8~mu\$ </tex-math </inline-formula> m With Fe:ZnSe Saturable Absorber. IEEE Photonics Technology Letters, 2019, 31, 565-568.	2.5	14
83	Visible-Wavelength All-Fiber Mode-Locked Vortex Laser. Journal of Lightwave Technology, 2022, 40, 191-195.	4.6	13
84	Fiber-optic parametric amplifier and oscillator based on intracavity parametric pump technique. Optics Letters, 2009, 34, 214.	3.3	12
85	Compact self-Q-switched, tunable mid-infrared all-fiber pulsed laser. Optics Express, 2018, 26, 34497.	3.4	12
86	Numerical analysis and optimization of optical spectral characteristics of fiber Bragg gratings modulated by a transverse acoustic wave. Applied Optics, 2007, 46, 6959.	2.1	11
87	Generation of optical frequency combs in a fiber-ring/microresonator laser system. Optics Letters, 2016, 41, 2576.	3.3	11
88	Externally Pumped Photonic Chipâ€Based Ultrafast Raman Soliton Source. Laser and Photonics Reviews, 2021, 15, 2000301.	8.7	11
89	Direct generation of orthogonally polarized dual-wavelength continuous-wave and passively Q-switched vortex beam in diode-pumped Pr:YLF lasers. Optics Letters, 2019, 44, 5586.	3.3	11
90	Mid-infrared all-fiber gain-switched pulsed laser at 3 μm. Opto-Electronic Advances, 2020, 3, 190032-190032.	13.3	11

#	Article	IF	CITATIONS
91	Ultrawide-Space and Controllable Soliton Molecules in a Narrow-Linewidth Mode-Locked Fiber Laser. IEEE Photonics Technology Letters, 2018, 30, 1423-1426.	2.5	10
92	3ÂW average-power high-order mode pulse in dissipative soliton resonance mode-locked fiber laser. Nanophotonics, 2021, 10, 3527-3539.	6.0	10
93	Effects of Nanomaterial Saturable Absorption on Passively Mode-Locked Fiber Lasers in an Anomalous Dispersion Regime: Simulations and Experiments. IEEE Journal of Selected Topics in Quantum Electronics, 2018, 24, 1-9.	2.9	9
94	Visible-Wavelength All-Fiber Vortex Laser. IEEE Photonics Technology Letters, 2019, 31, 1487-1490.	2.5	9
95	Visible Raman and Brillouin lasers from a microresonator/ZBLAN-fiber hybrid system. Photonics Research, 2019, 7, 566.	7.0	9
96	Towards Power Scaling of Simple CW Ultraviolet via Pr: LiYF ₄ -LBO Laser at 320 nm. IEEE Photonics Technology Letters, 2022, 34, 129-132.	2.5	8
97	Compact diode-pumped continuous-wave and passively Q-switched Nd:GYSO laser at 1.07 µm. Optics and Laser Technology, 2016, 82, 82-86.	4.6	7
98	Theoretical and Experimental Optimization of O-Band Multiwavelength Mixed-Cascaded Phosphosilicate Raman Fiber Lasers. IEEE Photonics Journal, 2011, 3, 633-643.	2.0	6
99	1.61–1.85 \$mu\$m Tunable All-Fiber Raman Soliton Source Using a Phosphor-Doped Fiber Pumped by 1.56 \$mu\$m Dissipative Solitons. IEEE Photonics Journal, 2017, 9, 1-7.	2.0	6
100	Ultra-high Q sphere-like cavities for cascaded stimulated Brillouin lasing. Optics Communications, 2017, 387, 421-425.	2.1	6
101	Optimizing the Self-Amplitude Modulation of Different 2-D Saturable Absorbers for Ultrafast Mode-Locked Fiber Lasers. IEEE Journal of Selected Topics in Quantum Electronics, 2019, 25, 1-10.	2.9	6
102	2166 nm all-fiber short-pulsed Raman laser based on germania-core fiber. Optics Express, 2019, 27, 34552.	3.4	6
103	Analytic modeling of the P-doped cascaded Raman fiber lasers. Optical Fiber Technology, 2007, 13, 22-26.	2.7	5
104	Low-threshold supercontinuum generation and optimization of PCF-intracavity-excited Q-switched fiber lasers. Optics Communications, 2014, 321, 145-149.	2.1	5
105	0.1–1-THz High-Repetition-Rate Femtosecond Pulse Generation From Quasi-CW Dual-Pumped All-Fiber Phase-Locked Kerr Combs. IEEE Photonics Journal, 2016, 8, 1-7.	2.0	5
106	Ultrafast Raman Fiber Laser Based on Cavity Matching Scheme and Heavily Germania-Core Fiber. Journal of Lightwave Technology, 2019, 37, 2914-2919.	4.6	5
107	Optimization of the multiwavelength erbium-doped fiber laser in a unidirectional cavity without isolator. Optical Fiber Technology, 2007, 13, 198-201.	2.7	4
108	Optimization of dual-wavelength cascaded Raman fiber lasers using an analytic approach. Optics Communications, 2007, 272, 414-419.	2.1	4

ZHENGQIAN LUO

#	Article	IF	CITATIONS
109	Continuously wavelength-spacing-tunable and idler-output multiwavelength fiber optical parametric oscillator. Optics Communications, 2011, 284, 2992-2996.	2.1	4
110	Passively Q-switched linear-cavity erbium-doped fiber laser with few-layer TI: Bi2Se3 saturable absorber. , 2014, , .		4
111	Intermode beating mode-locking technique for a rare-earth-doped fiber pulsed laser. Applied Optics, 2017, 56, 6103.	1.8	4
112	Visible-light all-fiber vortex lasers based on mode selective couplers*. Chinese Physics B, 2020, 29, 094204.	1.4	4
113	Visible-Wavelength-Tunable, Vortex-Beam Fiber Laser Based on a Long-Period Fiber Grating. IEEE Photonics Technology Letters, 2021, 33, 1173-1176.	2.5	4
114	Tunable, Continuous-Wave, Deep-Ultraviolet Laser Generation by Intracavity Frequency Doubling of Visible Fiber Lasers. Journal of Lightwave Technology, 2022, 40, 3900-3906.	4.6	4
115	2-μ4m wavelength all-fiber Q-switched double-clad fiber laser using monopiece single-layer chemical-vapor-deposition graphene. Optical Engineering, 2014, 53, 106103.	1.0	3
116	919.8Ânm self-Q-switched Nd-doped silica all-fiber laser. Optics Communications, 2020, 473, 125939.	2.1	3
117	800mW/1484nm highly efficient two-cascaded phosphosilicate Raman fiber laser pumped by Nd:YVO4 solid-state laser. Optics Communications, 2006, 265, 616-619.	2.1	2
118	Multiwavelength Fiber Lasers Based on SOA and Double-pass Mach-Zehnder Interferometer. , 2008, , .		2
119	Miniaturized Mid-Infrared All-Fiber Laser Passively Q-Switched by Topological Insulator Bi <inf>2</inf> Se <inf>3</inf> ., 2018, , .		2
120	1484-nm two-cascaded Raman fiber laser mode-locked by an intermode-beating mode-locking technique. Optical Engineering, 2015, 54, 046102.	1.0	1
121	Cascaded Brillouin, Raman, and Four-Wave-Mixing Generation in a 1.06-μm Microsphere-Feedback Yb-Fiber Laser. IEEE Photonics Journal, 2018, 10, 1-8.	2.0	1
122	Effects of nanomaterial saturable absorption on gain-guide soliton in a positive group-dispersion fiber laser: Simulations and experiments. Optics Communications, 2018, 406, 163-168.	2.1	1
123	On-chip mid-IR octave-tunable Raman soliton laser. Optics Express, 2022, 30, 25356.	3.4	1
124	High power LD-end-pumped Nd:YVO 4 laser as a pump source for Raman fiber laser. , 2007, , .		0
125	Theoretical and experimental investigation on backward-pumped Yb ³⁺ -doped double-clad fiber lasers. , 2008, , .		Ο
126	Novel L-band multiwavelength Raman fiber laser based on three-stage mixed-cascaded		0

#	Article	IF	CITATIONS
127	1212 nm high-efficiently-pumped 2 µm Tm/Ho-co-doped fiber laser Q-switched by graphene. , 2015, , .		0
128	1.63–1.73 µm tunable all-fiber femtosecond pulse generation from a P-doped Raman fiber pumped by 1.56 µm dissipative soliton. , 2016, , .		0
129	Compact visible Q-switching fiber lasers with transition-metal dichalcogenides. , 2017, , .		0
130	Intra-Cavity Mode-Selective Coupler Assisted Ultrafast Cylindrical Vector Fiber Laser. , 2019, , .		0
131	Intermodal-beating mode-locking: toward higher-order harmonic mode-locking of Raman laser. , 2012, ,		0
132	Modeling of mid-infrared fiber optical parametric oscillator. , 2012, , .		0
133	2-D materials-based passively Q-switched 635 nm Pr3+-doped ZBLAN fiber lasers. , 2015, , .		0
134	Novel Optical and Photonic Devices based on 2D Materials: feature issue introduction. Optical Materials Express, 2020, 10, 1344.	3.0	0
135	What makes the best chip-scale photonic sensor?. , 2020, , .		0
136	On-chip supercontinuum generation in Ge28Sb12Se60 chalcogenide waveguides and numerical investigation. , 2020, , .		0
137	Intracavity Frequency Doubling Deep-Ultraviolet Ho3+: ZBLAN Fiber Laser with Wavelength Tuning from 269.5 to 275.4 nm. , 2021, , .		0